THE *HUBBLE SPACE TELESCOPE* SURVEY OF BL LACERTAE OBJECTS. III. MORPHOLOGICAL PROPERTIES OF LOW-REDSHIFT HOST GALAXIES

RENATO FALOMO

Osservatorio Astronomico di Padova, Vicolo dell'Osservatorio 5, 35122 Padova, Italy

RICCARDO SCARPA[1]

Space Telescope Science Institute, 3700 San Martin Drive, Baltimore, MD 21218

ALDO TREVES

Università dell'Insubria, via Lucini 3 Como, Italy

AND

C. MEGAN URRY

Space Telescope Science Institute, 3700 San Martin Drive, Baltimore, MD 21218

ABSTRACT

We report on the optical properties of a sample of 30 BL Lac host galaxies in the redshift range $0.03 < z < 0.2$, as derived from *Hubble Space Telescope* observations. All galaxies are fully resolved in the WFPC2 (F702W filter) images, allowing a quantitative analysis in two dimensions. Most and possibly all of these galaxies have characteristics very similar to those of "normal" giant ellipticals. The luminosity, ellipticity, isophote twisting, and amount of disky or boxy isophotes are consistent with those found in nonactive ellipticals and in radio galaxies. In all cases the BL Lac nucleus is well centered in the main body of its host galaxy, a result that argues strongly against the microlensing hypothesis for any significant fraction of the population. A search for faint substructures in the host galaxies has not revealed notable signatures of tidal distortions or subcomponents (faint disks, bars, X features, etc.), and with only one exception, there are no prominent dusty features in the central regions. Instead, the BL Lac host galaxies are smooth and unperturbed, suggesting that strong external gravitational interactions are not important to ongoing activity. A careful examination of the environment around the nucleus, however, shows a high incidence of close companion objects, whose nature remains unclear pending spectroscopic observations.

Subject headings: BL Lacertae objects: general — galaxies: interactions — galaxies: structure

1. INTRODUCTION

The *Hubble Space Telescope* (*HST*) snapshot imaging survey of BL Lac objects[2] has produced a large, homogeneous data set of over 100 high-resolution images for the study of the environments of BL Lac nuclei. The targets were drawn from various samples and include sources in a wide range of redshift (z from 0.03 to ~1.4) as well as objects with unknown z. Results from the survey are given in Scarpa et al. (2000, hereafter Paper I) and Urry et al. (2000, hereafter Paper II). Previous *HST* imaging of BL Lac objects had been done only for a small number of sources (see Falomo et al. 1997; Jannuzi et al. 1997; Urry et al. 1999) but demonstrated the capabilities of *HST* for studying the environs of BL Lac objects.

The *HST* snapshot images have two main advantages with respect to ground-based images (e.g., Falomo 1996; Wurtz, Stocke, & Yee 1996; Falomo & Kotilainen 1999): an order of magnitude improved spatial resolution and very good homogeneity of data. On the other hand, the snapshot images were obtained with relatively short exposure times (typically minutes) and therefore are not very deep. This sets limits to the detection of very faint extended features, a well-known problem for *HST* images (see Falomo & Kotilainen 1999 for a direct comparison of *HST* and ground-based images of BL Lac objects).

Our first papers on the overall properties of the BL Lac objects derived from *HST* data focused on the determination of the absolute magnitude, scale length, and type of the host galaxies, as well as the luminosity of the nuclear source (see Paper II). This was based on accurate decomposition of the azimuthally averaged luminosity radial profiles, which allowed the study of the sources down to surface brightness $\mu_R \approx 25$ mag arcsec^{-2}. Additional morphological properties of the surrounding nebulosity, such as ellipticity, isophotal twisting, isophote shape (disky vs. boxy), presence of dust, etc., can only be derived from a full two-dimensional approach, which is possible for a subset of bright nearby host galaxies.

For elliptical galaxies it has been shown that isophote shapes are related to internal kinematics and to the radio and X-ray emission properties (e.g., Bender, Döbereiner, & Möllenhoff 1987). Moreover, significant distortions of the isophotes and/or twisting may be produced by strong galaxy interactions and/or merger events. It is therefore of interest to investigate these observable features in the galaxies hosting BL Lac nuclei in order to understand the (possible) role of galaxy structure on the nuclear activity. This kind of analysis has been performed so far only for a small number of nearby BL Lac objects (e.g., Falomo 1991, 1996; Heidt et al. 1999) because the presence of the bright nucleus often hinders a fully detailed morphological study.

---

[1] Also at Department of Astronomy, Padova University, Vicolo dell'Osservatorio 5, 35122 Padova, Italy.

[2] Based on observations made with the NASA/ESA *Hubble Space Telescope*, obtained at the Space Telescope Science Institute, which is operated by the Association of Universities for Research in Astronomy, Inc., under NASA contract NAS 5-26555.

In this paper we present the results of a two-dimensional analysis for 30 nearby ($z \lesssim 0.2$) snapshot BL Lac objects, i.e., those with the highest signal-to-noise ratios and the largest extent (see Table 1). For 25 of the 110 objects observed in the *HST* snapshot survey (Paper I) the redshift is unknown. Of these, 17 are spatially unresolved and are therefore most probably at $z > 0.2$. For the remaining eight resolved objects with unknown redshift, based on the apparent magnitudes of the nebulosities (see Paper I) and assuming that the luminosity of the host is consistent with that of other snap BL Lac objects (see Fig. 1), one expects that at most a few can be at $z < 0.2$. Therefore, the objects discussed here represent practically the totality of $z < 0.2$ BL Lac objects from our original sample of 110 objects.

For these low-z objects it is possible with *HST* to investigate features and structures in the host galaxy that are undetectable with ground-based observations. The host galaxy can be investigated down to less than 1 kpc from the nucleus (corresponding to 0″.3 at $z = 0.2$). In particular, one can search for slight off-centering of the nucleus with

respect to the galaxy, determine the presence of sub-components in the host galaxy, investigate the detailed shape of the isophotes, and search for dusty features and close companions.

Because the two broad components in BL Lac spectral energy distributions (SEDs) have peak power outputs (νL_ν) at wavelengths that increase systematically with luminosity (e.g., Ulrich, Maraschi, & Urry 1997), BL Lac objects found in radio and X-ray surveys have generally different SEDs. Radio-selected objects tend to have SEDs peaking at infrared–optical wavelengths and in the MeV–GeV gamma-ray band (low-frequency–peaked BL Lac objects, or LBLs) and exhibit luminosities approaching those of quasars. In contrast, X-ray–selected BL Lac objects have SEDs peaking at UV–X-ray wavelengths and again at TeV energies (high-frequency–peaked BL Lac objects, or HBLs) and are generally less luminous. Of the 30 sources in the present study, six are of LBL type, the rest being HBLs (Padovani & Giommi 1995). In the following analysis we have not addressed whether morphological properties are different for the two

TABLE 1
STRUCTURAL PROPERTIES OF LOW-REDSHIFT HOST GALAXIES

Name	z	ϵ[a]	C_4[b]	δ[c] (deg)	Δ[d] (arcsec)	$\Delta\theta$[e] (deg)
0145+138......	0.124	0.09	−0.40	0.04	0.05	22.0
0229+200......	0.139	0.16	−0.50	0.02	0.03	10.0
0347−121......	0.188	0.03	0.30	0.03	0.06	...
0350−371......	0.165	0.25	−1.20	0.02	0.02	5.0
0521−365......	0.055	0.30	0.00	0.02	0.04	4.0
0548−322......	0.069	0.20	−0.01	0.03	0.04	12.0
0706+591......	0.125	0.15	−0.80	0.02	0.04	16.0
0806+524......	0.137	0.08	1.20	0.03	0.05	...
0829+046......	0.180	0.10	0.20	0.04	0.04	...
0927+500......	0.188	0.24	0.60	0.03	0.04	7.0
1104+384......	0.031	0.19	0.00	0.03	0.04	15.0
1136+704......	0.045	0.04	0.00	0.01	0.01	...
1212+078......	0.136	0.04	−0.10	0.01	0.01	...
1218+304......	0.182	0.11	−1.50	0.04	0.05	23.0
1229+643......	0.164	0.16	−0.30	0.02	0.03	12.0
1255+244......	0.141	0.09	0.60	0.02	0.03	...
1418+546......	0.152	0.30	−0.30	0.02	0.02	15.0
1426+428......	0.129	0.33	−0.30	0.02	0.03	3.0
1440+122......	0.162	0.20	1.40	0.03	0.01	10.0
1514−241......	0.049	0.02	0.20	0.02	0.03	...
1728+502......	0.055	0.06	0.40	0.01	0.01	...
1807+698......	0.051	0.05	−0.80	0.02	0.04	...
1853+671......	0.212	0.15	0.40	0.05	0.04	30.0
1959+650......	0.048	0.20	1.50	0.03	0.07	17.0
2005−489......	0.071	0.26	0.80	0.03	0.05	12.0
2200+420......	0.069	0.25	−0.90	0.02	0.05	4.0
2201+044......	0.027	0.06	−0.60	0.05	0.00	...
2326+174......	0.213	0.12	−0.90	0.04	0.03	23.0
2344+514......	0.044	0.24	−0.60	0.02	0.02	5.0
2356−309......	0.165	0.25	0.70	0.04	0.07	6.0

[a] Ellipticity of the host galaxy at the effective radius. Typical error ± 0.02 far from the nucleus.

[b] Fourier coefficient $100C_4$ describing the isophote shape (see text); typical uncertainty is 0.5.

[c] Relative displacement of isophotes (dimensionless; see definition in § 3.3); typical uncertainty is ± 0.01.

[d] Off-centering of the nucleus with respect to the host galaxy (see definition in § 3.3); typical uncertainty is 0″.05.

[e] Maximum observed twisting of isophotes; measured only for host galaxies with $\epsilon > 0.1$.
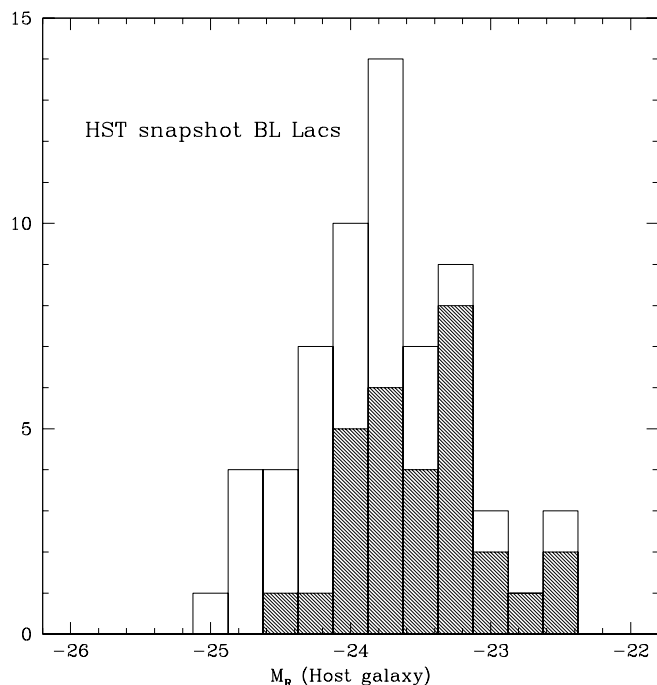
FIG. 1.—Distribution of host galaxy absolute magnitudes for the full *HST* snapshot sample (Paper II). *Hatched area*: Low-redshift subsample discussed in this paper.

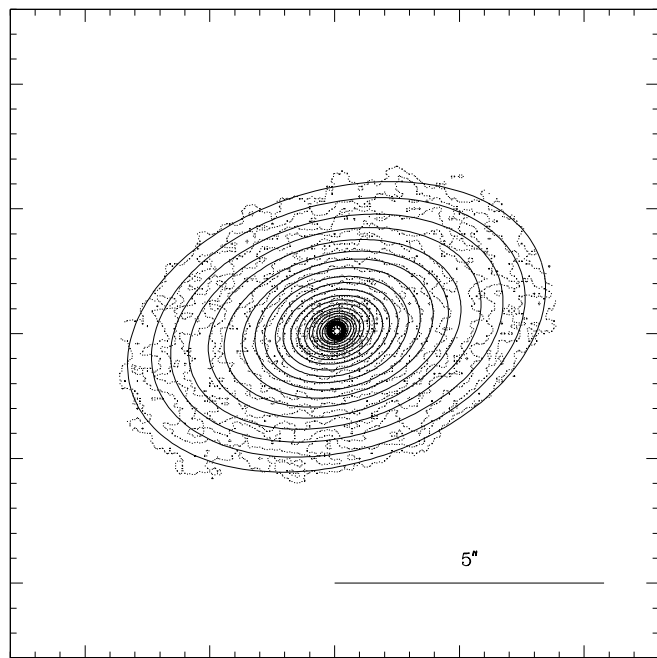FIG. 2.—Isophotes derived from the surface photometry analysis (*dotted lines*) and fitted ellipses (*solid lines*) for the BL Lac object 1426+428.

types of BL Lac objects, having found from our earlier analysis that the overall host galaxy characteristics do not depend on type (Paper II).

In § 2 we briefly describe the observations and our data analysis. Section 3 gives the results on the host galaxies' properties and shows the comparison with nonactive ellipticals and radio galaxies. Finally, in § 4 we summarize the results and draw the main conclusions from this study. Throughout the paper we used $H_0 = 50$ km s^{-1} kpc^{-1} and $q_0 = 0$.

2. OBSERVATIONS AND DATA ANALYSIS

The snapshot observations of BL Lac objects have been described in detail in Paper I; therefore, only the main steps are reviewed here. All objects considered here were observed with the WFPC2 camera of *HST* in the F702W filter. Each final image was obtained from the combination of typically three exposures for a total integration time of about 5–20 minutes (see Table 1 in Paper I for details). The point-spread function (PSF) used is a combination of a model derived from the Tiny Tim package (Krist 1995) plus a diffuse exponential tail that accounts for the first-order scattered light (see Urry et al. 1999 and Paper I for details). Photometric calibration was taken from Holtzman et al. (1995).

We performed a two-dimensional surface photometry analysis using an interactive numerical mapping package (AIAP; Fasano 1994), which produces an isophotal map of the image. This map was masked in order to avoid regions contaminated by companion objects, diffraction spikes, and any other extraneous features visible in the images. The isophotes were then fitted with ellipses down to $\mu_R = 22$–23 mag arcsec^{-2} (see Fig. 2 for an example). There are five geometric free parameters per isophote: semimajor axis (a), center position, ellipticity (ϵ), and position angle (P.A.),

which allow us to characterize the morphological and the photometric properties of the galaxy.

From this analysis we then derived the average position angles and ellipticity as a function of the generalized radius, $r = a(1 - \epsilon)^{1/2}$, and investigated their dependence on r (isophote twisting and ellipticity profiles). In addition, we examined the possible displacement of the centers of isophotes and the centering of the nucleus with respect to the galaxy.

3. RESULTS

3.1. *Luminosity Profiles and Two-dimensional Modeling*

For each object we derived a luminosity profile from the two-dimensional isophotal analysis and compared with that derived from the azimuthal average reported in Paper I. This was possible down to $\mu_R \approx 22$–23 mag arcsec^{-2}, since the fainter outer regions are too noisy to be investigated with the isophotal map. For all sources we find that the luminosity profile derived from the fit with ellipses of the isophotes is always in excellent agreement with that extracted from the azimuthal average (see example in Fig. 3).

We also fitted the isophotes with a two-dimensional galaxy model (either a de Vaucouleurs law or an exponential disk) convolved with the PSF plus a point source modeled by a scaled PSF. In all cases the de Vaucouleurs law gives a better fit to the data than the exponential disk model, in agreement with Papers I and II. This result is supported by the lack of spiral structures seen in the WFPC2 images and by the *diskiness* of the isophotes (see discussion in the following paragraphs). Absolute magnitudes and scale lengths of the host galaxies derived from the two-dimensional fitting are also in excellent agreement with the results of one-dimensional profile fitting (Paper I) and are consistent with the results from our deep *HST* images for a small number of BL Lac objects (Falomo et al. 1997).
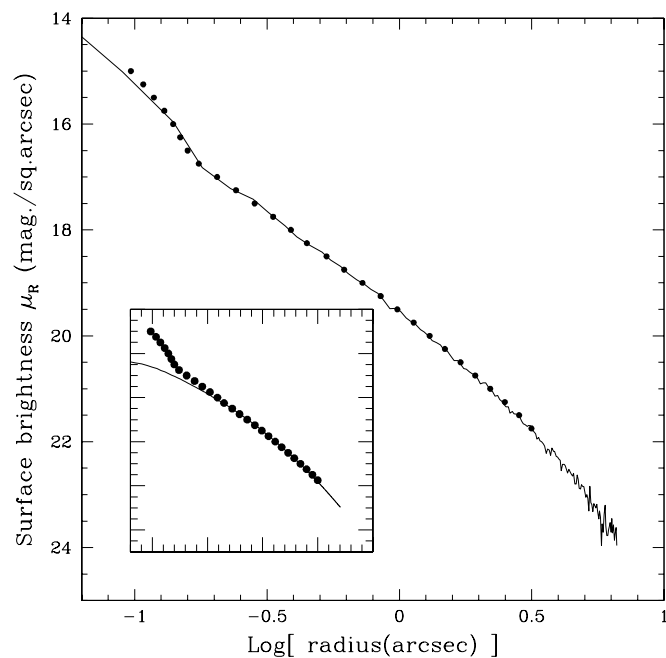
FIG. 3.—Radial surface brightness distribution of the BL Lac object 1426+428 derived from the two-dimensional analysis (*filled circles*), which agrees very well with the azimuthally averaged one-dimensional profile (*solid line*). The inset shows the brightness profile (*filled circles*) compared with the de Vaucouleurs fit (*solid line*). The excess at small radii is due to the presence of the bright nucleus (see Paper I for details).

3.2. *Ellipticity*

Since the ellipticity ϵ is in general dependent on the distance from the galaxy center, we report its value at the effective radius. However, because of the relatively high surface brightness limit, in some objects the ellipticity at the effective radius is not measurable, and in these cases we took the maximum ellipticity.

The values of ϵ are reported in Table 1. The error on observed ϵ for isophotes far from the nuclear regions is typically 0.02 (see Fasano & Bonoli 1990 for discussion). We show in Figure 4 the distribution of ellipticity for our 30 low-redshift BL Lac objects compared with that of 200 nearby normal (radio-quiet) ellipticals (Fasano & Vio 1991) and of a sample of 79 low-redshift radio galaxies (Govoni et al. 2000). Both normal ellipticals and radio galaxies exhibit the same ellipticity distribution: $\langle\epsilon\rangle_{\mathrm{Ell}} = 0.22 \pm 0.13$ and $\langle\epsilon\rangle_{\mathrm{RG}} = 0.21 \pm 0.12$. The average ellipticity for BL Lac hosts, $\langle\epsilon\rangle_{\mathrm{BLL}} = 0.16 \pm 0.09$, is slightly smaller than that of nonradio ellipticals and radio galaxies but is still consistent with being drawn from the same population ($P_{\mathrm{KS}} \sim 0.1$).

3.3. *Isophotal Displacement and Nuclear Decentering*

Displacement of isophotes with respect to the center may represent either a global distortion of the host galaxy, as a result of recent tidal interactions with close companions (e.g., Aguilar & White 1986), or a consequence of gravitational microlensing (Ostriker & Vietri 1985). In the first case one would expect nonconcentric isophotes to exhibit an asymmetry of distribution. To quantify this asymmetry we have computed the dimensionless parameter $\delta \equiv [(X_c - X_0)^2 + (Y_c - Y_0)^2]^{1/2}/r$, where X_c, Y_c are the centers of isophotal ellipses, (X_0, Y_0) is the location of the nucleus, and r is the radial distance to the particular elliptical isophote
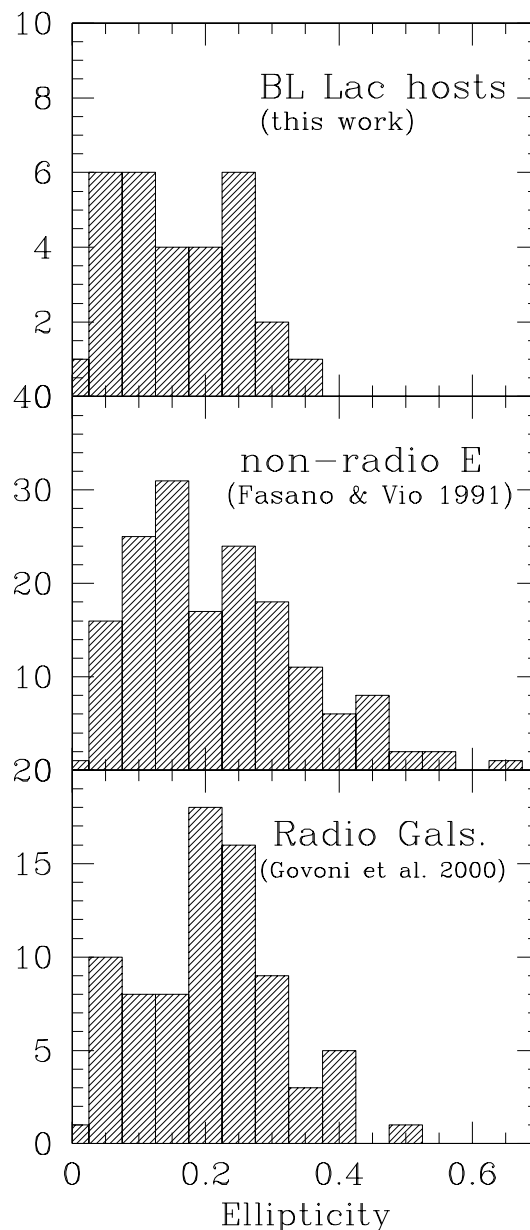

FIG. 4.—Comparison of the distribution of ellipticities for the host galaxies of BL Lac objects (*top*) with those of normal ellipticals (*middle*) from a sample of nearby galaxies (Fasano & Vio 1991) and low-redshift radio galaxies (*bottom*) (Govoni et al. 2000).

(defined earlier). Since δ may slightly change with r, we took the value at the effective radius R_e of the galaxy, or if R_e is beyond our measurements, we took the average value excluding the values at $r < 1''$.

In Figure 5 we show the distribution of δ derived from our sample of low-redshift BL Lac objects compared with that of radio galaxies from Govoni et al. (2000). The average value for our sample is $\langle\delta\rangle_{\mathrm{BLL}} = 0.027 \pm 0.01$ (median δ is 0.030), marginally consistent with zero but suggestive of small distortions in the galaxy isophotes. This is similar to the value reported for low-z radio galaxies, $\langle\delta\rangle_{\mathrm{RG}} = 0.03 \pm 0.04$ (Govoni et al. 2000), using a homogeneous procedure, while for 40 normal ellipticals observed by Sparks et al. (1991) from the ground, Colina & de Juan (1995) give $\langle\delta\rangle_{\mathrm{Ell}} = 0.02$ (see in Govoni et al. 2000 discussion and com-
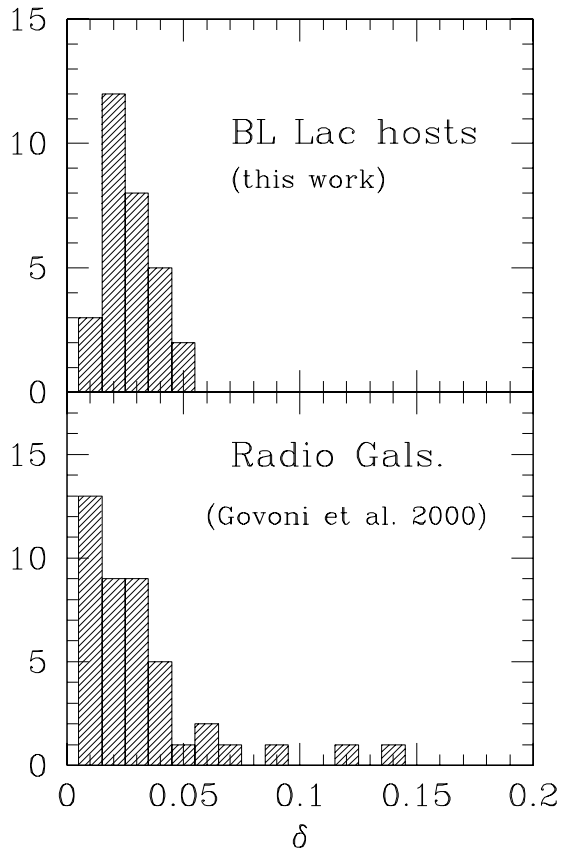
FIG. 5.—Comparison of the isophote displacement, δ (see text), for host galaxies of BL Lac objects (top) (present work) and low-redshift radio galaxies (bottom) (Govoni et al. 2000).

parison with other samples of radio galaxies). This is consistent with the idea that galaxies hosting BL Lac nuclei and/or radio sources have indistinguishable structures and have undergone a similar degree of interaction.

In the microlensing scenario (Ostriker & Vietri 1985, 1990), what appears to be the host galaxy is actually an intervening galaxy whose stars are microlensing a background quasar. Since the alignment will not be perfect, the galaxy will generally be off-center with respect to the point source, typically by $\gtrsim 0''.5$ (Merrifield 1992). To investigate this possibility, we computed for each object the limit of off-centering, $\Delta = |(x, y)_{\rm PSF} - (x, y)_{\rm gal}|$, comparing the PSF location with that of the galaxy (derived by averaging of isophotal centers after subtraction of a scaled nuclear point source and exclusion of the central circle of radius $0''.5$). With HST images the off-centering can be computed with unprecedented accuracy given the significantly better spatial resolution. The centers of nucleus and the host galaxy have a typical uncertainty of 0.2 and 0.4 pixels, respectively, so the net uncertainty is typically $\sim 0''.05$.

None of the objects in our (low-redshift) sample show significant ($> 2\sigma$) displacement of the point source with respect to the galaxy (values of Δ are given in Table 1); the observed displacements are always less than $0''.1$ and therefore consistent with zero off-centering. Since the low-redshift BL Lac objects were the prime candidates for microlensing according to Ostriker & Vietri (1985), our result strongly rules out the microlensing hypothesis for BL Lac objects in general.

3.4. Isophotal Twisting

For each host galaxy having ellipticity larger than 0.15 we have estimated the isophote twisting, $\Delta\theta$, computing the difference of position angles over the whole range of observed surface brightness (see Table 1). For the others the small ellipticity introduces large errors on the position angle so that it is not possible to get a reliable measurement of the isophotal twist.

The largest observed twist is $\sim 30°$ in $1853 + 671$; this value is, however, uncertain because of the relatively small ellipticity and short exposure time. We found five other objects (corresponding to $\sim 20\%$ of the sample) with isophote twists larger than $15°$. This is consistent (see Fig. 6) with what was found for a sample of 43 isolated (normal) ellipticals (Fasano & Bonoli 1989) and for 79 low-redshift radio galaxies (Govoni et al. 2000) using the same method to derive ΔP.A.
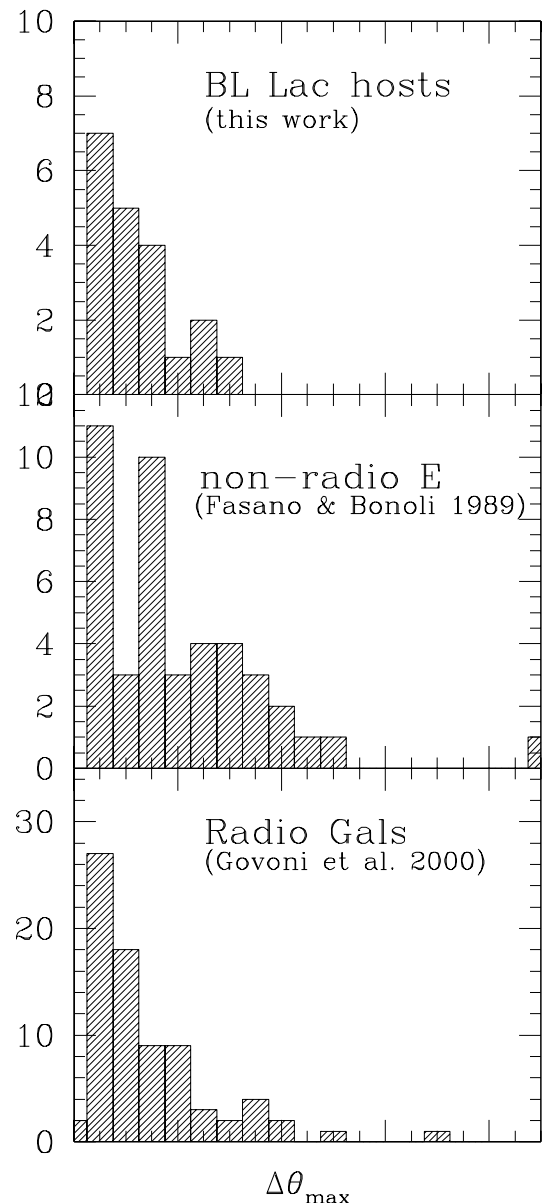

FIG. 6.—Comparison of the maximum isophotal twisting, $\Delta\theta_{\rm max}$, for BL Lac host galaxies (top), 43 nonradio elliptical galaxies (middle) (Fasano & Bonoli 1989), and low-redshift radio galaxies (bottom) (Govoni et al. 2000).

A small amount of isophote twisting may be explained simply by the triaxiality of the galaxies, while larger twists may be due to the effects of tidal interaction with companion galaxies (Kormendy 1982). The lack of large twists in our sample is consistent with the overall smoothness (unperturbed shape) of the host galaxies.

3.5. Isophotal Shapes: Disky and Boxy

To check for small deviations from purely elliptical isophotes, we analyzed the amplitude of the fourth cosine component, C_4, of the Fourier fit to the isophotes (e.g., Bender & Saglia 1999). A significant positive value of C_4 corresponds to *disky*-shaped isophotes, while a negative value indicates a *boxy*-shaped structure.

We found that 80% of the sources show a C_4 amplitude (at the effective radius) smaller than 1%, while no object exhibits $|C_4|$ larger than 3%. The distribution of C_4, shown in Figure 7, is symmetric around zero (mean value $\langle C_4 \rangle_{BLL} = 0.03\%$, rms dispersion 0.7%), and since the size of the error is around 0.5%, we conclude that in these galaxies there is no systematic deviation of isophotal shape from a simple ellipse. Similar distributions are observed in a sample of low-redshift radio galaxies using the same method ($\langle C_4 \rangle_{RG} = 0.04\% \pm 1.2\%$; Govoni et al. 2000) and also for radio galaxies in rich clusters (Ledlow & Owen 1995), as well as for normal ellipticals (Jorgensen, Franx, & Kjaergaard 1995).

3.6. Structures in the Host Galaxies

A first look at the raw images of BL Lac objects as well as the surface photometry analysis above indicate that galaxies hosting BL Lac objects are rather smooth and unperturbed (see images in Paper I). However, faint substructures could be hidden by the smooth contribution of the stellar component, so we subtracted a two-dimensional model of the galaxy using the best-fit parameters from the surface photometry analysis. This procedure enhances faint structures such as companions, jetlike features, or any other high-contrast feature superposed onto the image of the galaxy (e.g., Faundez-Abans & de Oliveira-Abans 1998 and references therein). Clearly, any region masked out during isophotal analysis (including the diffraction pattern of PSF spikes) will come out from this procedure. Moreover, because of the sharpness of the nucleus and the insufficient sampling of the PC, it was not possible to model the PSF adequately with this technique and some residuals (typically diffraction spikes) remain close to the nucleus. This has very little impact on our conclusions since structures very close to the nucleus are not considered.

In Figure 8 we show three examples of the images of the BL Lac objects before (*left panels*) and after (*right panels*) subtraction of the galaxy model. The top panels show the optical jet of PKS 0521−36 after subtraction of the galaxy–plus–point-source model. The middle panels show the image of the BL Lac object itself (2200+420), which, after subtraction of the model, does not exhibit significant features. Finally, the bottom panels show an example (H2356−309) of a companion at $\sim 1''$ southwest of the nucleus. In all three subtracted images the emission from the diffraction spikes (not modeled) is clearly visible.

The BL Lac objects in the present sample span the redshift range $0.03 \lesssim z \lesssim 0.2$. The usable field of view of the PC corresponds thus to a projected linear size of ~ 25–135 kpc. At *HST* resolution, therefore, we are practically able to
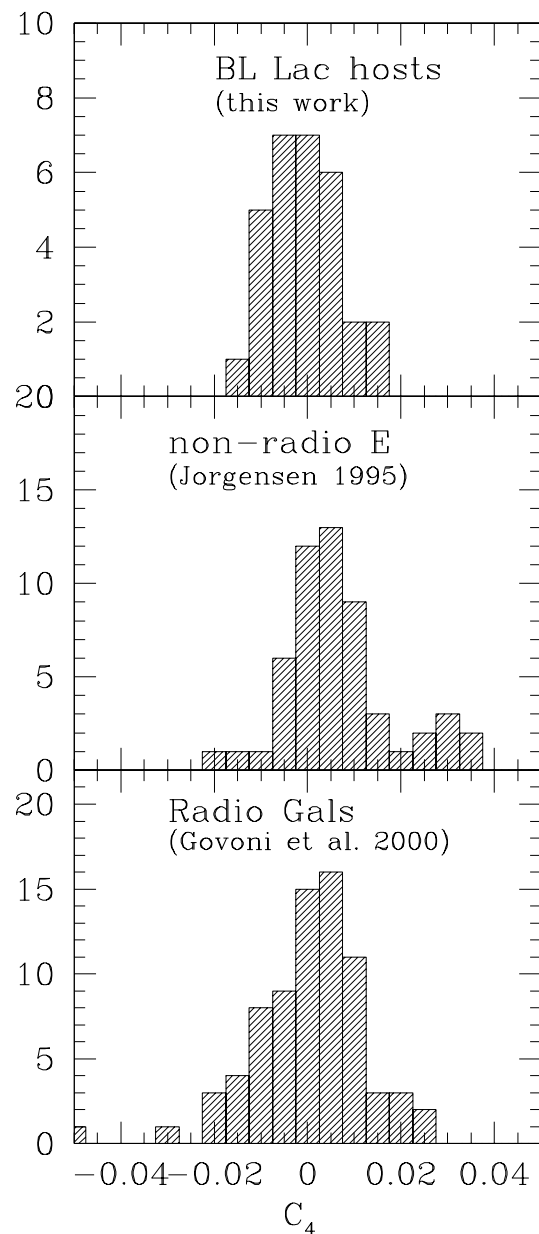

FIG. 7.—Comparison of the C_4 parameter (see text) for BL Lac host galaxies (*top*), normal ellipticals and S0 galaxies (*middle*) (Jorgensen et al. 1995), and low-redshift radio galaxies (*bottom*) (Govoni et al. 2000). The distributions are similar and consistent with little or no diskiness or boxiness.

explore structures in the host galaxies as close as 0.2–0.9 kpc (depending on z) to the nucleus (we assume that within 5 pixels from the center the signal is strongly dominated by the nuclear point source).

In three cases (0521−36, 3C 371, and 2201+044) an optical jet is clearly visible (see Scarpa et al. 1999b for a detailed study of these objects). One object (0806+524) has arclike emission at $\sim 2''$ from the nucleus, which could be a shell around the galaxy, a feature not uncommon among ellipticals (see Scarpa et al. 1999a for details). No other faint structures (shells, bars, or X-shaped features) are detected in the observed sources.

HST observations of nearby radio galaxies have shown that dusty features are present in the central regions of most
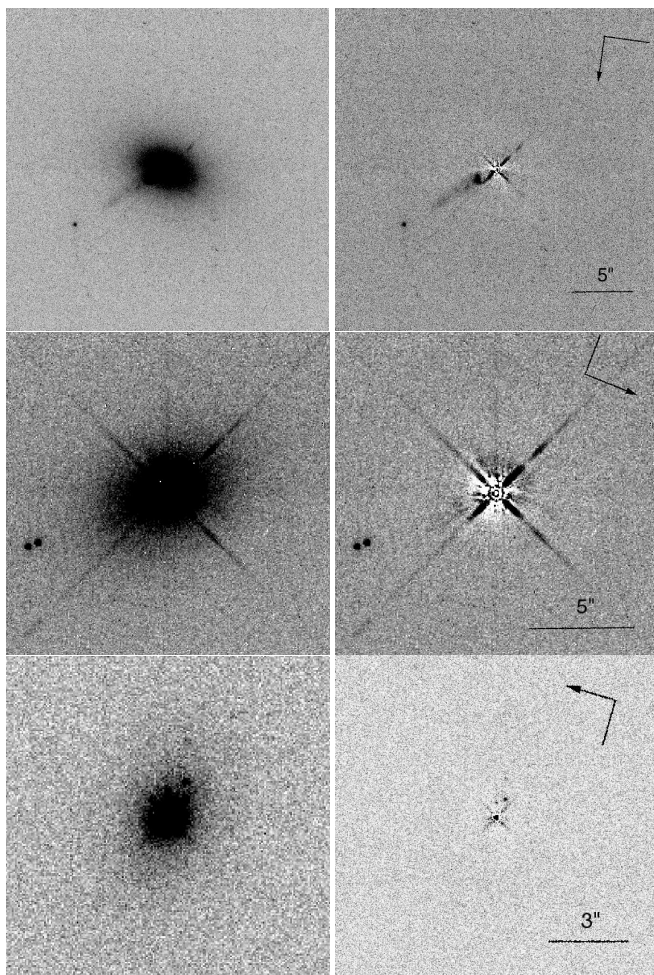
Fig. 8.—Example images of low-redshift *HST*-observed BL Lac objects (*left panels*) compared to galaxy-model–subtracted images (*right panels*). Both sides are displayed using the same grey scale. *Top:* PKS 0521−365 and its optical jet and bright knot ∼2″ from the nucleus. *Middle:* BL Lac object (2200+420). No significant residuals are detected after subtraction of the model (point source plus elliptical galaxy, convolved with the PSF). *Bottom:* H2356−309. A compact companion is detected 1″.2 from the nucleus of the galaxy. The cross-shaped residuals are due to the diffraction pattern of the *HST* PSF, which is not fully described by the two-dimensional modeling. Field orientation (*arrows mark north*) and scale are given for each image.

of the observed objects (Kleijn et al. 2000). These features often take the form of disks or lanes, but sometimes the distribution is irregular. The observed dust pattern is generally confined within a region typically less than 1.5 kpc (in most cases the physical sizes of disks and lanes range from 0.3 to 1.5 kpc). Since BL Lac objects are believed to be radio galaxies with the jet pointing toward us, we should observe similar dusty features also in our objects. However, two difficulties make this detection less likely in our sample objects. First, the bright nucleus tends to outshine the central regions of the host galaxy. Second, the average distance of our objects is larger than that of comparison samples of radio galaxies observed with *HST*, making the angular size of dusty features smaller. At $z = 0.05$, 1 kpc corresponds to ∼0″.75; at this distance from the center the light from the nucleus is normally fainter than that from the host galaxy (see Fig. 1 in Paper I), so that these features

could in principle be observable at the very lowest redshift but become progressively more difficult to detect at higher z.

In order to explore this possibility, we have therefore considered only the nine objects at $z < 0.1$ and searched for dusty features in the central regions after subtraction of the bright point source from the original image. In only one object (1959+650), which is at redshift $z = 0.048$, is a significant dust lane observed at ∼0″.8 (corresponding to ∼1 kpc) north of the nucleus and roughly aligned with the major axis of the galaxy. This feature was also noted by Heidt et al. (1999) on ground-based images and is discussed in our previous work (Scarpa et al. 1999a) on peculiar objects observed in the snapshot survey. For the rest of the eight $z < 0.1$ sources no clear signature of dust is found. Note that four of these objects are at a redshift similar to or smaller than that of 1959+650. This lack of detection suggests that the relevance of dusty features may be different in BL Lac objects and radio galaxies, with the caveat of the small statistics considered. Moreover, note that looking at features close to the nucleus requires not only high spatial resolution but also a PSF with sufficient sampling and faint wings. *HST* with the new Advanced Camera for Surveys High-Resolution Camera offers 2 times better sampling and has a coronagraph that depresses the PSF wings by factors of a few (and obscures the central 0″.9), so it could contribute to elucidating this point.

4. CLOSE COMPANIONS

In a number of objects we noted the presence of faint companions around the target, a feature that seems also common to the *HST* images of quasars. We have systematically explored the near environments of the 30 low-redshift BL Lac sources with the aim of identifying potential companion objects. For three cases (0706+592, 1440+122, and 2356−309) a very close ($\Delta < 1″.2$) compact companion is detected. These companions are located at projected distances of the order of 1–5 kpc from the nucleus. For five other BL Lac objects (see Table 2) diffuse or compact companions are found within a projected distance of ≲20 kpc (if they are at the same redshift as the BL Lac object).

In order to evaluate the statistical significance of the occurrence of these close companions, we derived the expected number of objects within a given radius from the BL Lac object based on the number counts observed in our PC frames well away from the BL Lac object. The observed average density of objects with $19.5 < m_R < 23.5$ mag is 9 ± 5 arcmin^{-2}, in good agreement with the observed galaxy density in several high latitude fields (Metcalfe et al. 1991).

At these faint magnitudes the counts at high Galactic latitudes are dominated by galaxies. The average Galactic latitude of our fields is $|b| = 45°$, but two fields (2200+420, 2344+514) are at low Galactic latitude ($|b| \sim 10°$), and one (1514−241) is at $|b| \sim 27°$ but close to the direction toward the Galactic center. The observed average density of stellar (unresolved) objects including all PC frames is 3.2 ± 4.2 arcmin^{-2}, while excluding the three fields mentioned above yields a star density of 2.1 ± 2.6 arcmin^{-2}. This is consistent with other estimates of the stellar density at high Galactic latitude (Hintzen, Romanishin, & Valdes 1991; Metcalfe et al. 1991).

Assuming the observed average density of faint ($19.5 < m_R < 23.5$ mag) objects, 9 arcmin^{-2}, around 30 targets, we

TABLE 2
Properties of Close Environments of BL Lac Objects

Name	Feature	m_R (mag)	M_R^a (mag)	Δ^b (arcsec kpc^{-1})	P.A.^{c} (deg)
0521−365......	Optical jet	19.9	...	1.8/2.7	∼305
0706+592......	Compact companion	24.8	−15	1.14/3.5	170
0829+046......	Companion galaxy	19.9	−20.5	4.9/20	145
1229+645......	Companion galaxy	19.2	−20.9	3.4/13	210
...	Compact companion	21.3	−18.8	4.5/17	3
1426+428......	Compact companion	21.7	−17.9	3.9/12	15
1440+122......	Companion galaxy	16.7	−23.4	2.5/9.4	260
...	Compact companion	19.5	−20.6	0.3/1.1	70
1959+650......	Dust lane	...	...	1.2/1.6	∼20
1807+698......	Optical jet	21.7	...	3.1/4.2	∼210
1853+671......	Companion galaxy	21.8	−18.9	2.1/9.8	323
2005−489......	Diffuse companion	22.7	−15.5	8.5/15.6	15
2201+044......	Optical jet	24.2	...	2.1/1.6	∼315
2326+174......	Compact companion	23.2	−17.5	3.2/15	150
2356−309......	Compact companion	22.5	−17.3	1.2/4.6	113

^{a} Absolute magnitude assuming the same redshift as the BL Lac object.
^{b} Projected distance from the nucleus assuming the same redshift as the BL Lac object.
^{c} Position angle of the feature.

would expect to find 0.06 companions at $r < 0\farcs5$, while one (a compact companion at $0\farcs3$ from 1440+122) is observed (Poisson probability $P = 0.06$). Within $1\farcs5$ we would expect to observe 0.6 objects, while three are detected ($P = 0.02$). At larger radii ($r < 5''$) we observe 11 companions when six are expected ($P = 0.02$). To test the reality of this apparent excess, we counted the number of detected objects within these same radii for random positions in each PC frame. In those cases we found 0, 1, and 7 companions, respectively, in agreement with the expected numbers of faint field objects.

Although the numbers are small and consequently the statistics are not very good, we conclude from our analysis that there is some indication that an association between BL Lac objects and companions is not dominated by chance alignments.

The identity or role of these companions is not yet clear, however. In other BL Lac fields, optical spectroscopy of the companion has sometimes proved the physical association with the active galaxy (Falomo 1996); in other cases, they have proved to be stars or foreground or background galaxies, fortuitously aligned with the BL Lac object (e.g., Stickel et al. 1991). For most cases here, spectra of the companion objects are not available and only statistical arguments suggest that some are likely associated with the BL Lac object.

Some of the close companions are resolved faint galaxies with absolute magnitudes (assuming they are at the distance of the BL Lac object) in the range $-21 < m_R < -19$ mag (Table 2). This is consistent with previous evidence that BL Lac objects inhabit environments with higher than average galaxy densities, as in groups or poor clusters (Pesce, Falomo, & Treves 1995; Wurtz et al. 1996). In the two cases with more than one companion, 1229+645 and 1440+122, the two companion objects are clearly different from one another, one being resolved and the other unresolved.

We note that a significant number of the observed companions are compact and appear pointlike even at *HST* resolution. Based on the counts of Galactic stars, we would expect only one or two chance alignments with stars, while six compact companions are observed (Table 2). The excess of compact companions is in fact more significant than the

excess of resolved companions (galaxies), especially since none of the compact sources belong to the low Galactic latitude fields where the star density is higher than the average value.

The nature of these unresolved companions is unclear. If they were at the redshift of the BL Lac object, their magnitudes would be in the range $-18 < m_R < -15$ mag, too luminous for globular clusters. These magnitudes are consistent with dwarf ellipticals, but the observed sources are probably too compact, unless they contain weak active nuclei (but they would have to be very weak indeed). One can ask whether some of these compact sources could be supernovae (SNe) of Type Ia. The SN Ia rate in early-type galaxies is estimated to be about 0.1–0.2 SNe/100 yr/10^{10} $L_\odot^B$ (Cappellaro, Evans, & Turatto 1999). This means that in a massive galaxy of $M_R \sim -23.7$ mag we expect to have about 1–2 SNe/100 yr. Because the SNe Ia at maximum reach $M_R \approx -19.4$ mag and our limiting magnitude for stellar objects is $m_R \sim 24.5$ mag (it is $m_R \sim 24$ mag for extended objects), at $z \sim 0.1$ we should be able to detect such SNe for about 100 days. Therefore, we should find 0.2 SNe in our 30 galaxies observed. Unless the SN rate in these active galaxies is significantly higher than the average for normal ellipticals, it is highly unlikely that the compact companions are SNe.

We believe the nature of all these companions, resolved or unresolved, will remain uncertain until spectroscopy is performed. Whatever their identity, there is little evidence of tidal interaction in the BL Lac host galaxy (appreciable isophote twisting, nonconcentric isophotes, etc.), which suggests that the companions are not strongly perturbing it. Gravitational interactions might have had a greater role in the past in the formation and fueling of the active nucleus, and what we see now could be a leftover of an earlier (close) interaction. One interesting possibility suggested by numerical simulations (Bekki 1999) is that the close companions are the product of a past major merger between gas-rich galaxies and also provide fuel for the nuclear activity but are not necessarily linked to the formation of a massive black hole in the nucleus or to the sustenance of an active relativistic jet.

5. SUMMARY AND CONCLUSIONS

We have presented detailed morphological analysis of *HST* images for 30 galaxies hosting BL Lac sources at redshift $z \lesssim 0.2$. The galaxies were investigated with an order of magnitude better spatial resolution than is possible from the ground.

Our analysis indicates that in spite of the presence of the active nucleus, the host galaxy appears in most cases to be a completely "normal" elliptical. Both the ellipticity and the isophotal shape distributions are similar to those for radio galaxies and radio-quiet ellipticals. This suggests that tidal interactions are very infrequent or are short-lived with respect to the nuclear activity timescale.

We find no indication of displacement and/or off-centering of the galaxy isophotes with respect to the nucleus, meaning that the unresolved nuclear source truly sits in the center of the galaxy. This rules out the microlensing hypothesis for BL Lac objects, which predicts frequent off-centering of the nucleus. This does not exclude the possibility that some objects could be lensed (see Scarpa et al. 1999a), but it cannot be a widespread explanation of the BL Lac phenomenon.

An interesting result is the finding of excess close companions in several cases. A high incidence of companions of BL Lac objects was first suggested by Falomo, Melnick, & Tanzi (1991) from subarcsecond-resolution ground-based imaging and was later confirmed by Pesce et al. (1995), Falomo (1996), and Heidt et al. (1999). Close companions seem also to be common around quasars imaged by *HST* (Bahcall et al. 1997; Disney et al. 1995).

REFERENCES

Aguilar, L. A., & White, S. D. M. 1986, ApJ, 307, 97
Bahcall, J. N., Kirhakos, S., Saxe, D. H., & Schneider, D. P. 1997, ApJ, 479, 642
Bekki, K. 1999, ApJ, submitted (astro-ph/9904044)
Bender, R., Döbereiner, S., & Möllenhoff, C. 1987, A&A, 177, L53
Bender, R., & Saglia, R. P. 1999, in ASP Conf. Ser. 182, Galaxy Dynamics, ed. D. R. Merritt, M. Valluri, & J. A. Sellwood (San Francisco: ASP), 113
Cappellaro, E., Evans, R., & Turatto, M. 1999, A&A, 351, 459
Colina, L., & de Juan, L. 1995, ApJ, 448, 548
Disney, M. J., et al. 1995, Nature, 376, 150
Falomo, R. 1991, AJ, 101, 821
———. 1996, MNRAS, 283, 241
Falomo, R., & Kotilainen, J. 1999, A&A, 352, 85
Falomo, R., Melnick, J., & Tanzi, E. G. 1990, Nature, 345, 692
Falomo, R., Urry, C. M., Pesce, J. E., Scarpa, R., Giavalisco, M., & Treves, A. 1997, ApJ, 476, 113
Fasano, G. 1994, Padova Observatory Internal Rep.
Fasano, G., & Bonoli, C. 1989, A&AS, 79, 291
———. 1990, A&A, 234, 89
Fasano, G., & Vio, R. 1991, MNRAS, 249, 629
Faundez-Abans, M., & de Oliveira-Abans, M. 1998, A&AS, 128, 289
Govoni, F., Falomo, R., Fasano, G., & Scarpa, R. 2000, A&A, 353, 507
Heidt, J., Nilsson, K., Sillanpää, A., Takalo, L. O., & Pursimo, T. 1999, A&A, 341, 683
Hintzen, P., Romanishin, W., & Valdes, F. 1991, ApJ, 366, 7
Holtzman, J. A., Burrows, C. J., Casertano, S., Hester, J. J., Trauger, J. T., Watson, A. M., & Worthey, G. 1995, PASP, 107, 1065
Jannuzi, B., et al. 1997, ApJ, 491, 146
Jorgensen, I., Franx, M., & Kjaergaard, P. 1995, MNRAS, 273, 1097

Kleijn, G. A. V., Baum, S. A., de Zeeuw, P. T., & O'Dea, C. P. 2000, AJ, 118, 2592
Kormendy, J. 1982, in 12th Advanced Course of the Swiss Society of Astronomy and Astrophysics, Morphology and Dynamics of Galaxies, ed. L. Martinet & M. Mayor (Sauverny: Geneva Obs.), 113
Krist, J. E. 1995, in Calibrating *Hubble Space Telescope* Post Servicing Mission, ed. A. Koratkar & C. Leitherer (Baltimore: STScI), 311
Ledlow, M. J., & Owen, F. N. 1995, AJ, 109, 853
Merrifield, M. R. 1992, AJ, 104, 1306
Metcalfe, N., Shanks, T., Fong, R., & Jones, L. R. 1991, MNRAS, 249, 498
Ostriker, J. P., & Vietri, M. 1985, Nature, 318, 446
———. 1990, Nature, 344, 45
Padovani, P., & Giommi, P. 1995, ApJ, 444, 567
Pesce, J. E., Falomo, R., & Treves, A. 1995, AJ, 110, 1554
Scarpa, R., Urry, C. M., Falomo, R., Pesce, J. E., & Treves, A. 2000, ApJ, 532, 740 (Paper I)
Scarpa, R., Urry, C. M., Falomo, R. Pesce, J. E., Webster, R., O'Dowd, M., & Treves, A. 1999a, ApJ, 521, 134
Scarpa, R., Urry, C. M., Falomo, R., & Treves, A. 1999b, ApJ, 526, 643
Sparks, W. B., Wall, J. V., Jorden, P. R., Thorne, D. J., & van Breda, I. 1991, ApJS, 76, 471
Stickel, M., Fried, J. W., Kühr, H., Padovani, P., & Urry, C. M. 1991, ApJ, 374, 431
Ulrich, M.-H., Maraschi, L., & Urry, C. M. 1997, ARA&A, 35, 445
Urry, C. M., et al. 1999, ApJ, 512, 88
———. 2000, ApJ, 532, 816 (Paper II)
Wurtz, R., Ellingson, E., Stocke, J. T., & Yee, H. K. C. 1996, AJ, 106, 869
Wurtz, R., Stocke, J. T., & Yee, H. K. C. 1996, ApJS, 103, 109